

DOI: 10.1002/cssc.201300605

Physiological Stratification in Electricity-Producing Biofilms of *Geobacter sulfurreducens*

Germán David Schrott,^{*} María Victoria Ordoñez, Luciana Robuschi, and Juan Pablo Busalmen^[a]

The elucidation of mechanisms and limitations in electrode respiration by electroactive biofilms is significant for the development of rapidly emerging clean energy production and wastewater treatment technologies. In *Geobacter sulfurreducens* biofilms, the controlling steps in current production are thought to be the metabolic activity of cells, but still remain to be determined. By quantifying the DNA, RNA, and protein content during the long-term growth of biofilms on polarized graphite electrodes, we show in this work that current production be-

comes independent of DNA accumulation immediately after a maximal current is achieved. Indeed, the mean respiratory rate of biofilms rapidly decreases after this point, which indicates the progressive accumulation of cells that do not contribute to current production or contribute to a negligible extent. These results support the occurrence of physiological stratification within biofilms as a consequence of respiratory limitations imposed by limited biofilm conductivity.

Introduction

Gram negative bacteria from the *Geobacteriaceae* family can use extracellular compounds as final electron acceptors. In particular, *Geobacter sulfurreducens* is able to oxidize acetate to CO₂ while reducing extracellular insoluble Fe^{III} compounds as well as toxic metals and humic substances, among others, which thus transfers electrons to the extracellular medium.^[1] It has been demonstrated that extracellular final electron acceptors can be replaced by polarized electrodes, which allows the use of *G. sulfurreducens* cells for electricity production from the oxidation of dissolved organic matter.^[1b,2] This discovery rapidly prompted intensive research focused on bacteria–electrode communication as a way to improve practical applications in clean energy production and wastewater treatment.^[1b,3] *G. sulfurreducens* has been studied intensively as it can develop electrically conductive biofilms on the anode of microbial fuel cells (MFCs) to produce the highest current density ever reported for an electroactive bacteria.^[4] Indeed, the availability of its complete genome sequence,^[5] a tractable genetic system,^[6] and a genome-scale metabolic model^[7] have boosted its study (see Ref.[8] for a complete review of the topic).

A remarkable feature of electricity-producing biofilms is that cells located at tenths of micrometers from the electrode are still able to use it as the final electron acceptor,^[9] but the specific electron-transfer mechanisms that allow conduction remain unclear. Currently, a very active discussion is ongoing regarding two proposals: the electron hopping model,^[10] which states that electrons are transported through a series of

redox reactions that involve cytochromes located in the extracellular matrix that connect each cell to the electrode; and the metallic-like conduction model, according to which electrons move along proteinaceous conductive filaments (pilin nano-wires) that extend from the cell external membrane through the extracellular environment and to the electrode. Conductivity is proposed to be conferred in this case by electronic resonance between aromatic residues in the pili structure by π -stacking conduction.^[11]

The conductivity of the biofilm matrix is crucial to determine the physiological state of cells in the biofilm interior because, depending on their relative position from the electrode, cells can face a respiratory limitation.^[10a,e] If biofilm conductivities are taken into account in the order of those estimated from cyclic voltammetry results, a redox gradient is predicted to occur inside the biofilm as a consequence of the lack of oxidized electron carriers (heme groups in external cytochromes).^[10e] This gradient has been recently visualized in vivo by using confocal Raman microscopy,^[12] which evidenced the anticipated limitation on cell respiration. Indeed, it has been proposed that this limitation might ultimately compromise cell replication.^[10a,e-g] If, on the other hand, biofilm conductivity is as high as indicated by the direct measurements reported by Malvankar et al.,^[11] the potential decay within the biofilm height would be negligible (because of metallic-like behavior), which would not produce any limitation in the electron acceptor availability for any cell in the population and thus not limit growth.^[10e]

Physiological information can thus be significant to support one model or the other, but in the case of *Geobacter* biofilms it is still limited. Within the available data, a linear relationship was reported initially between the increment of the produced current and protein accumulation during biofilm growth,

[a] G. D. Schrott, Dr. M. V. Ordoñez, L. Robuschi, Dr. J. P. Busalmen
División Electroquímica y Corrosión INTEMA-CONICET-UNMdP
Juan B Justo 4302, B7608FDQ, Mar del Plata (Argentina)
E-mail: germans@fi.mdp.edu.ar

Supporting Information for this article is available on the WWW under <http://dx.doi.org/10.1002/cssc.201300605>.

1 which led to the conclusion that all cells in the biofilm respire
2 at the same rate^[9a] and to the expectation of a uniform distri-
3 bution of cell activity all over the biofilm. Later, evidence was
4 provided on the occurrence of physiological changes during
5 biofilm growth by showing the evolution of the electron-trans-
6 fer rate (i.e., the current per mg of protein).^[9c] It was demon-
7 strated that the cells that attached and duplicated initially had
8 a lower respiration rate than those that supported exponential
9 growth, but unfortunately data were only collected up to the
10 late exponential phase of growth when a maximal current
11 output was reached (i.e., approximately 100 h of growth),
12 which left the biofilm physiology virtually unexplored beyond
13 that point. More recently, data have been obtained about post-
14 exponential growth,^[12] which show that current production be-
15 comes independent of biofilm thickness once the biofilms are
16 60–70 μm thick, and, more importantly, it has been shown that
17 biofilms continue to grow after that point to reach up to
18 120 μm in thickness, which raises questions about the physio-
19 logical balance within biofilm cells that could explain these re-
20 sults.

21 With the aim to gain an insight into biofilm physiology
22 during long-term growth, in this work we determined DNA,
23 RNA, and protein contents over the development of biofilms
24 of *G. sulfurreducens* in a continuous culture, which covered
25 more than 350 h of growth. By correlating the data obtained
26 to the current production, we were able to confirm that cur-
27 rent production becomes independent of DNA accumulation
28 once a maximal current is reached. The results indeed show
29 that *G. sulfurreducens* biofilms continue to grow after reaching
30 the point of maximum current production, but exhibit a fast
31 reduction in the mean respiratory rate after the late exponen-
32 tial phase, in agreement with the progressive accumulation of
33 cells that do not contribute to current production, or contrib-
34 ute to a negligible extent.

35 Of great importance for the identification of the biofilm con-
36 duction mechanism, the results presented here are in accord-
37 ance with the occurrence of redox gradients (i.e., physiological
38 stratification) in the biofilm interior and can be explained by
39 considering a base layer of active cells (approximately 30–
40 50 μm thick) that promotes the growth of the biofilm towards
41 the solution side in which less active cells are progressively ac-
42 cumulated, which lowers the mean metabolic activity of the
43 population. According to previous reports,^[10a,e–g,11,12] for this in-
44 terpretation to be valid, biofilm electron conduction may oper-
45 ate by electron hopping.

47 Results and Discussion

48 The growth of *G. sulfurreducens* biofilms has typically been
49 evaluated through the measurement of the produced current
50 in chronoamperometric experiments. The application of this
51 method is supported by the reported linear correlation be-
52 tween current and biomass (i.e., growth)^[9a] and in a typical
53 case allows the visualization of an exponential current increase
54 caused by the active reproduction of cells at maximal speed
55 while using the electrode as the electron acceptor. Under con-
56 tinuous-culture conditions, if biofilms reach a thickness of ap-

proximately 60 μm , the current becomes stationary,^[9b,12,13]
which evidences a change in the developmental process of the
population that is often interpreted as the beginning of sta-
tionary growth. Nevertheless, it is actually inferred only from
current production data because biochemical information
shows that the evolution of biofilms beyond this point is still
lacking.

With the aim to gain information about biological variables
that influence the current production beyond the point of cur-
rent stabilization, we simultaneously determined current pro-
duction and the content of DNA, RNA, and proteins during the
development of *G. sulfurreducens* biofilm in continuous culture
for up to 300 h after the maximum current was reached. This
was performed under a high concentration of buffer and an
excess of electron donor to prevent limitations owing to local
acidification and the lack of carbon source,^[10e,13c,14] respectively.
Under these conditions, our current data were consistent with
those typically found by others (Figure S1A),^[9c,13a,14c,15] but
were followed by the development of a macroscopically visi-
ble, pink-colored biofilms on the polarized electrodes (Fig-
ure S1B). Interestingly, from data shown in Figures S1A and B
it becomes evident that the strong pink color appeared over
the electrode surface well after the stabilization of the current,
which indicates that the thickness of the biofilms continued to
increase for 300 h after the maximal current was attained. The
final average thickness of our biofilms was approximately
350 μm , determined by direct measurement with a conductive
microelectrode (see the Supporting Information for a detailed
explanation of the technique). More importantly, our results
and those of Robuschi et al.^[12] evidence that biofilm maturity
may not be directly related to the stabilization of current pro-
duction^[9b,c,13b,16] and reveal the possibility to increase the bio-
film power output provided that a method is found to recruit
otherwise idle cells in the upper layers.^[12]

The voltammetric profile determined over the growth of bio-
films was the same as that described by others (Figure S2A),
which includes noncatalytic signals superimposed on a promi-
nent turnover process that corresponds to the catalysis of ace-
tate oxidation. In addition, nonturnover voltammetry results
(Figure S2B) were similar to those already reported by others,
which allowed both the estimation of a midpoint potential of
approximately -0.15 V [vs. the standard hydrogen electrode
(SHE)] for the main biofilm redox process and the confirmation
of a linear correlation between the height of the redox peaks
and the square root of the scan rate, indicative of diffusive
control on the charge transfer process^[9c,15,17] (Figure S2B).
These results confirm that the controlling steps in the electric-
ity production process do not change over the complete bio-
film development for up to 350 h.

The growth measured as DNA accumulation gives a more
detailed insight into the process of biofilm maturation and
shows that, in agreement with the results in Figure S1, DNA ac-
cumulates almost constantly during more than 120 h beyond
the point when the current production reaches its maximum
(Figure 1); indeed, the DNA content increased sixfold in this
period. These results indicate the progressive accumulation of
cells that do not contribute to current production or contrib-

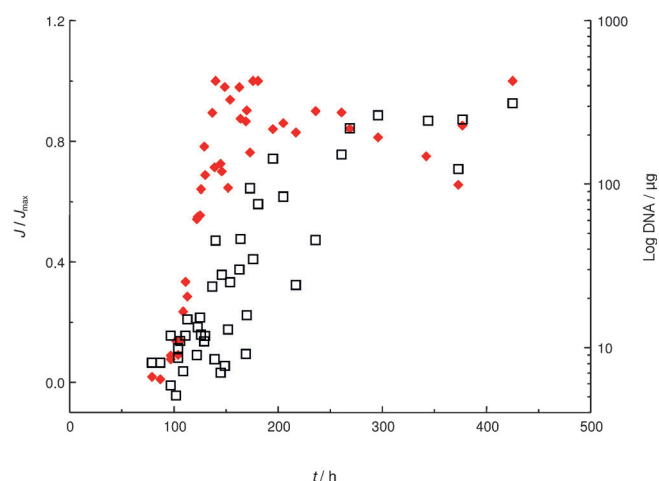


Figure 1. Correlation between growth and current production in electrogenic biofilms. Biofilms of *G. sulfurreducens* were developed anaerobically on graphite electrodes polarized at 0.4 V (vs. SHE) as the unique electron acceptor and acetate (20 mM) as the carbon source. Normalized current density (\blacklozenge) and DNA content (\square) along electrogenic biofilm development are shown. Biomass samples were collected at different times after inoculation. Normalized current density was calculated from chronoamperometric data as: $J [A m^{-2}]/J_{max} [A_{max} m^{-2}]$ and plotted versus $t [h]$. The maximum current density obtained was $6.63 \pm 0.81 A m^{-2}$. For each sample, the DNA content was quantified by Fleck and Munro's protocol and plotted on a logarithmic scale versus $t [h]$. Values correspond to five independent experiments.

ute to a negligible extent and are compatible with the occurrence of some physiological stratification. This phenomenon is now well established in non-electroactive biofilms because of the formation of microdomains in which cells may present different metabolic activities,^[18] but data available in the particular case of *Geobacter* biofilms are limited and mostly refer to biofilms analyzed up to the late exponential phase. In spite of this, it is interesting to highlight that Franks et al.^[13b] have shown a lower abundance of ribosomal protein gene transcripts in the outer half of these biofilms, which suggests that cells in this region grow more slowly,^[13b] in line with the result presented here.

Physiological stratification can be explained if we take into account that imperfect conduction through the biofilm matrix leads to the progressive accumulation of electrons in the external cytochromes of cells located far from the electrode as first proposed by Strycharz-Glaven et al.^[10a] and later demonstrated by Robuschi et al.^[12] by using confocal Raman microscopy. According to calculations by Bonanni et al.,^[10e] this accumulation would impact negatively on the respiration rate of cells located beyond approximately 70 μm of the electrode, which would be then limited to respire at nearly their basal or maintenance rate,^[10e] thus unable to participate in further growth or current production. If these predictions are correct, the accumulation of biomass as a consequence of growth near the electrode may lead ultimately to a decrease in the mean respiratory rate of the entire population because of the increment of the number of cells pushed out of the 70 μm limit. To test this hypothesis, we related the current values obtained here to the content of total biofilm proteins as a way to estimate the mean electron-transfer rate (i.e., the respiratory rate) per unit

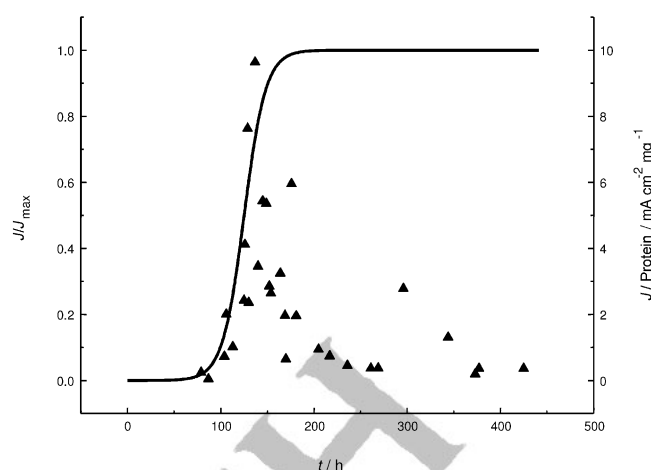


Figure 2. Respiration rate of electrogenic biofilms as a function of total protein content of the biofilm. *Geobacter* electrogenic biofilms were developed and samples were collected at different times after inoculation (see the Experimental Section). The protein content was quantified at each point following the bicinconinic acid protocol using BSA as standard. The respiration rate was calculated as current density output [$mA cm^{-2}$]/protein content [mg] and plotted versus $t [h]$. The left-hand y axis shows the typical normalized current density evolution registered for all biofilms used for macromolecular extraction ($n=52$).

mass of protein [$mA mg^{-1}$] of the entire population over time. According to the results shown in Figure 2, this rate increases with exponential growth to reach a maximum after approximately 120 h, but later decreases fast to a minimum of approximately 1.4 $mA mg^{-1}$ (Figure 2), which agrees closely with the calculations of Bonanni et al.^[10e] and with the respiratory rate reported for *Geobacter* cells that respire Fe^{III} at a maintenance regime.^[10e] The same trend is obtained for the estimation of the respiratory rate per cell by relating the current to the DNA content (Figure S3). Notably, the maximum current per DNA content or protein content ratio occurs approximately 48 h before the maximum current is attained (Figures 2 and S3), which evidences the early beginning of physiological stratification in accordance with data reported by Marsili et al.^[9c] and with the reduced gene expression for ribosomal proteins reported by Franks et al.^[13b]

The genetic flow of information in cells is from DNA to RNA synthesis and finally to protein production.^[19] As the amount of DNA per cell is relatively constant and the amount of RNA increases significantly during fast growth (mostly because of the accumulation of rRNA), to support the elevated synthesis of enzymes and proteins, the RNA/DNA ratio has been identified as a good indicator for the overall physiological state of cell cultures.^[20] In this direction, we calculated the mean RNA/DNA ratio for the biofilms studied here with the aim to evaluate the physiological changes along their developmental process. This ratio is directly related to gene expression and is typically higher if most cells in a culture are metabolically active and replicate at a high rate. In *G. sulfurreducens* cells, for example, an increased content of ribosomal proteins was found in faster growing cultures.^[21] Also, in the closely related *G. uraniireducens*, the transcript abundance for ribosomal protein genes was directly related to the growth rate.^[22] However, the

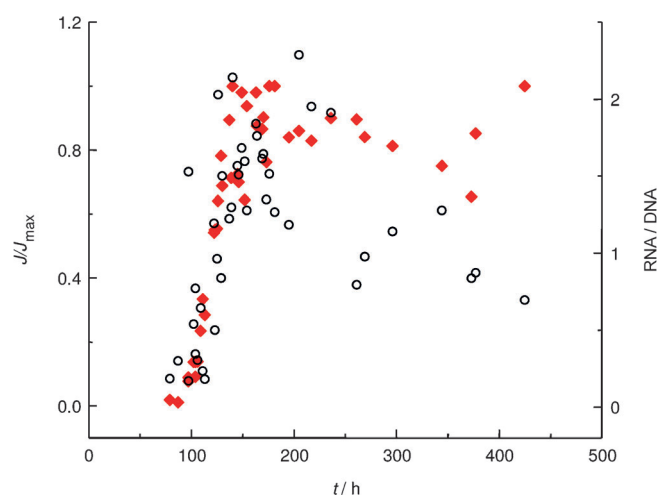


Figure 3. Changes in the net physiological state of electrogenic biofilms and its correlation with current output over time. *Geobacter* electrogenic biofilms were collected at increasing times from inoculation and processed to determine the metabolic state at each growth stage. The normalized current density and RNA/DNA ratio variations during biofilm development are shown. The content of nucleic acids was quantified as described (see the Experimental Section), and the RNA [μg]/DNA [μg] ratio (\circ) and J [mA cm^{-2}]/ J_{max} [$\text{mA}_{\text{max}} \text{cm}^{-2}$] (\blacklozenge) were calculated and plotted versus t [h]. Values correspond to five independent experiments.

RNA/DNA ratio is expected to decrease upon the occurrence of limitations to microbial activity. The data in Figure 3 show that in the case of the biofilms studied here, the mean RNA/DNA ratio rapidly increases during the first 120 h of growth, until a maximum of approximately 2 is reached at the time when current production was maximal. Beyond that point, the RNA/DNA ratio started to decrease, which evidences the occurrence of some limitation to the metabolic activity, in accordance with the stratification of cell activity discussed previously that is expected to occur in the upper biofilm layers. The final value of the RNA/DNA ratio was approximately 0.6 after 350 h (Figure 3), which typically indicates stationary growth.^[23] These results are in accordance with those presented by Franks et al.,^[13b] in which a decrease of the transcript levels of genes that encode for a number of ribosomal proteins was found in the upper half (25 μm) of a 55 μm thick *G. sulfurreducens* biofilm that reached maximum current. Moreover, they also found a small decrease in the transcript level of genes related to the tricarboxylic acid (TCA) cycle in the same biofilm region. Indeed, it has to be taken into account that the strategy used by these authors (by pooling the upper 25 μm of the biofilm) had probably hidden stronger variations that occur in higher biofilm layers.

In the comparison of data shown in Figures 2 and 3, attention is drawn to the fact that the RNA/DNA ratio decreases much more slowly than the respiratory rate, which suggests that, in spite of the respiratory limitation, some anabolic activity is maintained for a relatively long period of time. Although it cannot be explained based on the available information, it may be related to a response to the respiratory limitation, as the overproduction of external cytochromes reported in electron-acceptor-limited planktonic cells of *G. sulfurreducens*^[24] has

been demonstrated to improve the electroactivity of the cells.^[25]

To obtain additional information on the physiological state of cells within the biofilm layers, they were grown on an indium tin oxide (ITO) transparent electrode as the unique electron acceptor following procedures reported earlier.^[12] The electrochemical behavior in terms of current output and voltammetric fingerprint resembled that obtained on graphite, but ITO opened the possibility to evaluate the biofilm physiology and structure by using confocal microscopy in combination with live/dead staining. Based on data reported in Figures 1 and 2, the analysis was performed 20 h after the maximum current was reached. The results are shown in Figure 4

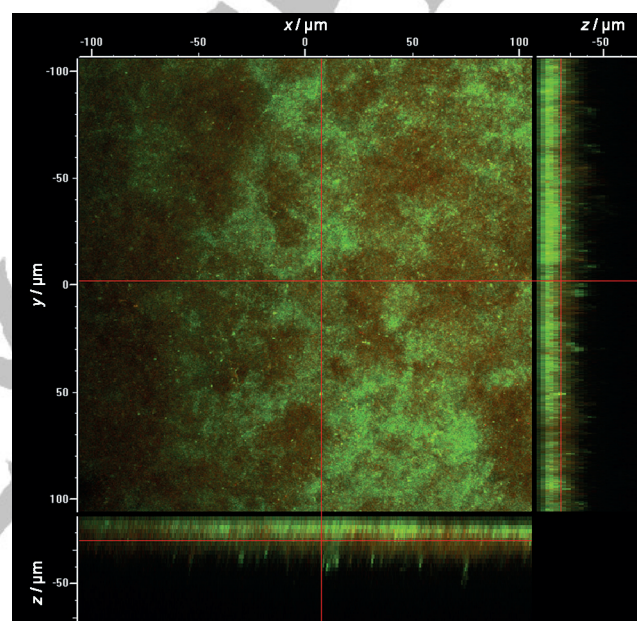


Figure 4. Confocal laser scanning micrograph of a *G. sulfurreducens* biofilm that produced a steady-state current treated with a live/dead viability stain. Bacteria with intact membranes appear stained in green, whereas bacteria with damaged membranes appear in red. Large panel: single slice through biofilm parallel to the electrode. Bottom and right panels: cross-sections indicated by red lines in the large panel. E: electrode.

and reinforce the occurrence of physiological stratification. Active cells with intact membranes were primarily detected at basal biofilm layers, in the first 30–40 μm from the anode surface. Those located beyond that limit, however, showed evidence of some membrane damage. These results are in agreement with those reported by Nevin et al.^[4] and support the hypothesis that states that cells in the upper part of the biofilm are most likely inactive/not growing and do not contribute to current production.

In summary, our data can be explained by considering that *G. sulfurreducens* biofilms are physiologically stratified and that current is produced by a small number of actively respiring and dividing cells, which are located close to the electrode surface. As a consequence of growth, these very active cells produce daughter cells that contribute to the increment of the biofilm thickness at a constant rate and push others towards

the solution side. As soon as cells are pushed away from a critical distance (i.e., 50–70 μm) from the electrode, their respiration rate becomes limited^[10e,12] and, consequently, they cannot continue to contribute to biofilm growth and current production. In the end, cells at the outermost layer of the biofilm cannot respire anymore because of the lack of an electron acceptor and they leave the biofilm to search for a most suitable site to live in. Implicit in this interpretation is the fact that biofilms can accumulate over five times the biomass required for maximal current production (Figure 1), which shows that the solution to conductivity limitations (i.e., respiratory limitations) may put the technology of microbial fuel cells over the sustainability limit, as previously calculated.^[10e]

Conclusions

We demonstrated that biofilms of *G. sulfurreducens* that grow on a polarized electrode become physiologically stratified beyond the late exponential phase of growth. Stratification was shown by the reduction in the RNA/DNA ratio and the mean respiratory rate of the population and evidenced the accumulation of cells that do not contribute to current production. Live/dead staining confirmed that physiologically depressed cells are located towards the solution side as expected from internal redox gradients reported recently. All of the results presented are in line with a limitation in the respiratory activity in upper layers of biofilms because of limited conduction through the extracellular matrix, which supports electron hopping as the operating conduction mechanism.

Experimental Section

Biological material and biofilm growth

Geobacter sulfurreducens strain DSM12127 was first anaerobically grown in batches at 32 °C on a medium prepared as described by Schrott et al.^[10c] that contained acetate (20 mM) and fumarate (40 mM). For biofilm production, this batch culture (10 mL) at early stationary phase was inoculated into a single-chamber three-electrode electrochemical cell that contained deoxygenated culture medium with acetate (20 mM) and no fumarate. The biofilms developed anaerobically over a 4 mm diameter and 25 mm length graphite rod and in a continuous culture. After 24 h of incubation in batch mode, a peristaltic pump was connected to continuously supply medium. The reactor and all liquid reservoirs in the continuous culture were permanently flushed with a gas mixture of N_2/CO_2 (80:20) to adjust the pH of the medium to 7.4 and prevent contamination by O_2 . All the experiments were performed at 32 °C under permanent magnetic stirring.

Cell setup and electrochemical assays

All the experiments were performed in an electrochemical cell using graphite rods as the working electrode, with eight working electrodes per reactor, polarized at a constant potential of 0.2 V vs. Ag/AgCl 3 M NaCl (0.4 V vs. SHE) reference electrode and with a Pt wire as a counter electrode. All electrochemical assays were performed by using a FRA2 $\mu\text{AUTOLAB}$ type III potentiostat controlled by 1.6 NOVA dedicated software.

Biofilm sample preparation

Graphite rods that contained biofilms were sampled from the electrochemical cell at different points of growth once the biofilms started to produce current (60–425 h after inoculation) and stored at –20 °C until use. Biofilm samples were detached from the electrode surface by centrifugation at 8000 $\times g$ for 15 min after immersing the complete rod in sample buffer (phosphate buffer 50 mM, NaCl 137 mM, and KCl 2.7 mM). Pellets that contained biofilm cells were used for the quantification of different macromolecules as described below. To corroborate that the biofilms were totally harvested, graphite rods were fixed in glutaraldehyde 2.5% for 15 min, dehydrated by immersion in an alcoholic series (40%, 60%, 80%, and 100% ethanol in ultrapure water), air-dried, and sputtered with gold for observation by SEM by using a Jeol JSM-6460LV electron microscope.

Quantification of macromolecules

The pellets obtained were subjected to Fleck and Munro's^[26] extraction protocol to obtain DNA, RNA, and protein hydrolyzed extracts. In brief, each biofilm was softly resuspended in Tris-HCl 100 mM pH 7.5 and centrifuged at 8000 $\times g$ for 15 min. The supernatant that contained extracellular biofilm material was separated, and the cellular integrity was corroborated in the collected pellets by live/dead staining. The pellet was resuspended in PCA (0.2 N) to promote cell disruption and centrifuged at 10 000 $\times g$ for 10 min to collect nucleic acids and proteins. The new pellet was resuspended in KOH (0.3 N) and hydrolyzed by heating at 40 °C for 40 min. After neutralizing with chilled PCA (0.5 N), soluble ribonucleotides were separated by centrifugation at 3000 $\times g$ for 10 min. The obtained pellet was resuspended in PCA (0.5 N) and incubated at 70 °C for 1 h to promote DNA hydrolysis and then centrifuged at 3000 $\times g$ for 10 min. The new supernatant was saved as total DNA, and the final pellet was resuspended in NaOH (3%, w/v) and used as the protein sample. The nucleic acid content was determined by spectrophotometry at 260 nm (conversion coefficient: 0.0309). The RNA/DNA ratio and current density/DNA ratio were calculated as metabolic state and respiratory rate per cell, respectively. The protein content was estimated by using the bicinonic acid method^[27] using bovine serum albumin (BSA) as the standard. The current/protein ratio was calculated and used as the electron-transfer rate for the biofilm over time. All ratios estimated from biochemical data were considered as a mean representation of the biofilm cell population.

Confocal microscopy

G. sulfurreducens biofilms were grown in an electrochemical cell as described elsewhere^[12] with ITO as the electron acceptor under the same growth conditions (buffer, temperature, pH, etc.) as described above. 20 h beyond the point at which the maximum current was reached, the biofilms were stained fluorescently by using a live/dead BacLight bacterial viability kit (Molecular Probes, Invitrogen) following manufacturer's instructions with some modifications: 1.5 μL of the dye mixture was added for each 1 mL of bacterial suspension. Incubation was performed in the dark by recirculation with a peristaltic pump for 30 min. After staining, the biofilms were examined by using a Nikon Eclipse C1 Plus confocal microscope controlled by EZ-C1 3.80 dedicated software, equipped with a 60 \times objective with a distance-correction ring (ULWD Nikon) and 488 and 561 nm filters.

Acknowledgements

The technical assistance of Juan Assarou and José Kochur from INTEMA is greatly acknowledged. This work was supported by the European Union through the BacWire FP7 Collaboration project (contract: NMP4-SL-2009-229337). G.D.S. and L.R. are doctoral fellows and M.V.O. is a postdoctoral fellow from CONICET, Argentina.

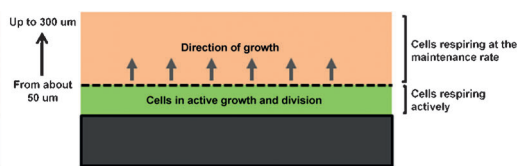
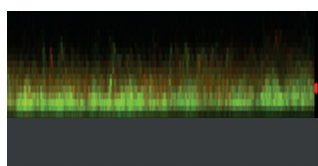
Keywords: biological activity · DNA · electrochemistry · energy conversion · fuel cells

- [1] a) J. W. Voordeckers, B.-C. Kim, M. Izallalen, D. R. Lovley, *Appl. Environ. Microbiol.* **2010**, *76*, 2371; b) D. R. Lovley, *Nat. Rev. Microbiol.* **2006**, *4*, 497.
- [2] D. R. Bond, D. R. Lovley, *Appl. Environ. Microbiol.* **2003**, *69*, 1548.
- [3] a) D. R. Lovley, K. P. Nevin, *Curr. Opin. Biotechnol.* **2011**, *22*, 441; b) B. E. Logan, K. Rabaey, *Science* **2012**, *337*, 686; c) H. Liu, R. Ramnarayanan, B. E. Logan, *Environ. Sci. Technol.* **2004**, *38*, 2281; d) B. E. Logan, *Nat. Rev. Microbiol.* **2009**, *7*, 375; e) B. K. Min, S. A. Cheng, B. E. Logan, *Water Res.* **2005**, *39*, 1675; f) K. Rabaey, W. Verstraete, *Trends Biotechnol.* **2005**, *23*, 291.
- [4] P. Nevin, H. Richter, S. F. Covalla, J. P. Johnson, T. L. Woodard, A. L. Orloff, H. Jia, M. Zhang, D. R. Lovley, *Environ. Microbiol.* **2008**, *10*, 2505.
- [5] B. A. Methe, K. E. Nelson, J. A. Eisen, I. T. Paulsen, W. Nelson, J. F. Heidelberg, D. Wu, M. Wu, N. Ward, M. J. Beanan, R. J. Dodson, R. Madupu, L. M. Brinkac, S. C. Daugherty, R. T. DeBoy, A. S. Durkin, M. Gwinn, J. F. Kolonay, S. A. Sullivan, D. H. Haft, J. Selengut, T. M. Davidsen, N. Zafar, O. White, B. Tran, C. Romero, H. A. Forberger, J. Weidman, H. Khouri, T. V. Feldblyum, T. R. Utterback, S. E. Van Aken, D. R. Lovley, C. M. Fraser, *Science* **2003**, *302*, 1967.
- [6] M. V. Coppi, C. Leang, S. J. Sandler, D. R. Lovley, *Appl. Environ. Microbiol.* **2001**, *67*, 3180.
- [7] R. Mahadevan, D. R. Bond, J. E. Butler, A. Esteve-Núñez, M. V. Coppi, B. O. Palsson, C. H. Schilling, D. R. Lovley, *Appl. Environ. Microbiol.* **2006**, *72*, 1558.
- [8] D. R. Lovley, *Energy Environ. Sci.* **2011**, *4*, 4896.
- [9] a) G. Reguera, K. P. Nevin, J. S. Nicoll, S. F. Covalla, T. L. Woodard, D. R. Lovley, *Appl. Environ. Microbiol.* **2006**, *72*, 7345; b) A. E. Franks, R. H. Glaven, D. R. Lovley, *ChemSusChem* **2012**, *5*, 1092; c) E. Marsili, J. Sun, D. R. Bond, *Electroanalysis* **2010**, *22*, 865.
- [10] a) S. M. Strycharz-Glaven, R. M. Snider, A. Guiseppe-Elie, L. M. Tender, *Energy Environ. Sci.* **2011**, *4*, 4366; b) Y. Liu, H. Kim, R. R. Franklin, D. R. Bond, *ChemPhysChem* **2011**, *12*, 2235; c) G. D. Schrott, P. S. Bonanni, L. Robuschi, A. Esteve-Núñez, J. P. Busalmen, *Electrochim. Acta* **2011**, *56*, 10791; d) P. S. Bonanni, G. Schrott, J. P. Busalmen, *Biochem. Soc. Trans.* **2012**, *40*, 1274; e) P. S. Bonanni, D. F. Bradley, G. Schrott, J. P. Busalmen, *ChemSusChem* **2013**, *6*, 711–720; f) D. R. Bond, S. M. Strycharz, L. Tender, C. I. Torres, *ChemSusChem* **2012**, *5*, 1099; g) Y. Liu, D. R. Bond, *ChemSusChem* **2012**, *5*, 1047; h) R. M. Snider, S. M. Strycharz-Glaven, S. D. Tsoi, J. S. Erickson, L. M. Tender, *Proc. Natl. Acad. Sci. USA* **2012**, *109*, 15467; i) S. Pirbadian, M. Y. El-Naggar, *Phys. Chem. Chem. Phys.* **2012**, *14*, 13802.
- [11] N. S. Malvankar, M. Vargas, K. P. Nevin, A. E. Franks, C. Leang, B.-C. Kim, K. Inoue, T. Mester, S. F. Covalla, J. P. Johnson, V. M. Rotello, M. T. Tuominen, D. R. Lovley, *Nat. Nanotechnol.* **2011**, *6*, 573.
- [12] L. Robuschi, J. P. Tomba, G. D. Schrott, P. S. Bonanni, P. M. Desimone, J. P. Busalmen, *Angew. Chem.* **2013**, *125*, 959; *Angew. Chem. Int. Ed.* **2013**, *52*, 925.
- [13] a) K. P. Nevin, B.-C. Kim, R. H. Glaven, J. P. Johnson, T. L. Woodard, B. A. Methé, R. J. DiDonato, Jr., S. F. Covalla, A. E. Franks, A. Liu, D. R. Lovley, *PLoS ONE* **2009**, *4*, e5628; b) A. E. Franks, K. P. Nevin, R. H. Glaven, D. R. Lovley, *ISME J.* **2010**, *4*, 509; c) A. E. Franks, K. P. Nevin, H. Jia, M. Izallalen, T. L. Woodard, D. R. Lovley, *Energy Environ. Sci.* **2009**, *2*, 113.
- [14] a) C. I. Torres, A. K. Marcus, B. E. Rittmann, *Biotechnol. Bioeng.* **2008**, *100*, 872; b) H.-S. Lee, C. s. I. Torres, B. E. Rittmann, *Environ. Sci. Technol.* **2009**, *43*, 7571; c) E. Marsili, J. B. Rollefson, D. B. Baron, R. M. Hozalski, D. R. Bond, *Appl. Environ. Microbiol.* **2008**, *74*, 7329.
- [15] a) S. M. Strycharz-Glaven, L. M. Tender, *ChemSusChem* **2012**, *5*, 1106; b) H. Richter, K. P. Nevin, H. Jia, D. A. Lowy, D. R. Lovley, L. M. Tender, *Energy Environ. Sci.* **2009**, *2*, 506.
- [16] G. Reguera, K. D. McCarthy, T. Mehta, J. S. Nicoll, M. T. Tuominen, D. R. Lovley, *Nature* **2005**, *435*, 1098.
- [17] a) S. M. Strycharz, A. P. Malanoski, R. M. Snider, H. Yi, D. R. Lovley, L. M. Tender, *Energy Environ. Sci.* **2011**, *4*, 896; b) K. P. Katuri, P. Kavanagh, S. Rengaraj, D. Leech, *Chem. Commun.* **2010**, *46*, 4758.
- [18] J. R. Lawrence, G. D. W. Swerhone, U. Kuhlicke, T. R. Neu, *Can. J. Microbiol.* **2007**, *53*, 450.
- [19] F. C. Neidhardt, J. L. Ingraham, M. Schaechter in *Physiology of the Bacterial Cell. A Molecular Approach*, Sinauer Associates Inc., Sunderland, **1990**, pp. 389.
- [20] H. Bremer, P. P. Dennis in *Escherichia coli and Salmonella typhimurium. Cellular and Molecular Biology, Vol. 2* (Eds.: F. C. Neidhardt, J. L. Ingraham, K. B. Low, B. Megasanik, M. Schaechter, H. E. Umarger), American Society for Microbiology, Washington, DC, **1987**.
- [21] Y.-H. R. Ding, K. K. Hixson, C. S. Giometti, A. Stanley, A. Esteve-Núñez, T. Khare, S. L. Tollaksen, W. Zhu, J. N. Adkins, M. S. Lipton, R. D. Smith, T. Mester, D. R. Lovley, *Biochim. Biophys. Acta Proteins Proteomics* **2006**, *1764*, 1198.
- [22] D. E. Holmes, R. A. O'Neil, M. A. Chavan, L. A. N'Guessan, H. A. Vronis, L. A. Perpetua, M. J. Larrahondo, R. DiDonato, A. Liu, D. R. Lovley, *ISME J.* **2009**, *3*, 216.
- [23] D. Nercessian, F. B. Duville, M. Desimone, S. Simison, J. P. Busalmen, *Water Res.* **2010**, *44*, 2592.
- [24] A. Esteve-Núñez, M. Rothermich, M. Sharma, D. Lovley, *Environ. Microbiol.* **2005**, *7*, 641.
- [25] A. Esteve-Núñez, J. P. Busalmen, A. Berna, C. Gutierrez-Garran, J. M. Feliu, *Energy Environ. Sci.* **2011**, *4*, 2066.
- [26] A. Fleck, H. N. Munro, *Biochim. Biophys. Acta Spec. Sect. Nucleic Acids Relat. Subj.* **1962**, *55*, 571.
- [27] P. K. Smith, R. I. Krohn, G. T. Hermanson, A. K. Mallia, F. H. Gartner, M. D. Provenzano, E. K. Fujimoto, N. M. Goeke, B. J. Olson, D. C. Klenk, *Anal. Biochem.* **1985**, *150*, 76.

Received: June 25, 2013

Revised: September 27, 2013

Published online on ■■■, 0000



G. D. Schrott,* M. V. Ordoñez, L. Robuschi,
J. P. Busalmen

■ ■ - ■ ■ ■

Physiological Stratification in
Electricity-Producing Biofilms of
Geobacter sulfurreducens

Live wire! Biochemical data reveal that biomass accumulation in electrogenic biofilms is fivefold higher than the one that supports maximal current production and that most cells in the biofilm

are physiologically limited, strongly suggesting that biofilms potentially put microbial fuel cells well beyond the sustainability threshold if internal conductivity limits are overcome.

WILEY-VCH
Galley Proofs